

Multiscale modeling of fiber reinforced materials via non-matching immersed methods

Giovanni Alzetta^a, Luca Heltai^a

^a*SISSA-International School for Advanced Studies
via Bonomea 265, 34136 Trieste - Italy*

Abstract

Fiber reinforced materials (FRMs) can be modeled as bi-phasic materials, where different constitutive behaviors are associated with different phases. The numerical study of FRMs through a full geometrical resolution of the two phases is often computationally infeasible, and therefore most works on the subject resort to homogenization theory, and exploit strong regularity assumptions on the fibers distribution. Both approaches fall short in intermediate regimes where lack of regularity does not justify a homogenized approach, and when the fiber geometry or their numerosity render the fully resolved problem numerically intractable.

In this paper, we propose a distributed Lagrange multiplier approach, where the effect of the fibers is superimposed on a background isotropic material through an independent description of the fibers. The two phases are coupled through a constraint condition, opening the way for intricate fiber-bulk couplings as well as allowing complex geometries with no alignment requirements between the discretisation of the background elastic matrix and the fibers.

We analyze both a full order coupling, where the elastic matrix is coupled with fibers that have a finite thickness, as well as a reduced order model, where the position of their centerline uniquely determines the fibers. Well posedness, existence, and uniqueness of solutions are shown both for the continuous models, and for the finite element discretizations. We validate our approach against the models derived by the rule of mixtures, and by the Halpin-Tsai formulation.

Keywords: Immersed boundary method, finite element method, fiber composites, Lagrange multipliers

1. Introduction

Numerous engineering applications require the efficient solution of partial differential equations involving multiple, complex geometries on different phases; *composite materials* are the prototypical example of such problems. During the past fifty years, the interest

Email addresses: giovanni.alzetta@sissa.it (Giovanni Alzetta), luca.heltai@sissa.it (Luca Heltai)

in composite materials flourished multiple times; it began for their applications to new materials in multiple fields, such as aerospace engineering [19], civil engineering [38], and materials science [6, 36].

During the nineties, the increasing importance of biomechanics in life sciences lead to the development of numerous models describing, e.g., arterial walls [27], soft tissues [25], and muscle fibers [28].

Recent years saw the rise of new application fields, such as the study of natural fiber composites [44], and engineering methods to accurately recover the three-dimensional structure of a material sample, e.g., [29, 30].

From the first studies on composites, it has been clear that their properties are strongly dependent on their internal structure: the volume ratio between each component, the orientation, the shape, all contribute substantially to the material’s properties [19, 20]. One of the most wide-spread and significant example of composites is that of Fiber Reinforced Materials (FRMs), where thin, elongated structures (the fibers) are immersed in an underlying isotropic material (the elastic matrix).

We may separate the approaches used to study FRMs into two broad groups: i) “*homogenization methods*”, which study a complex inhomogeneous body by approximating it with a fictitious homogeneous body that behaves globally in the same way [49], and ii) “*fully resolved*” methods, which use separate geometrical and constitutive descriptions for the elastic matrix and the individual fibers.

As examples of analytical “*homogenization methods*” we recall the rule of mixtures [18] and the *empirical* Halpin-Tsai equations [17], used to study a transversely isotropic unidirectional composite, where fibers are uniformly distributed and share the same orientation. The development of homogenization theory led, in recent years, to more complex models, e.g., [26, 5].

More intricate homogeneization approaches rely on numerical methods to provide a “cell” behaviour, which is then replicated using periodicity, using, e.g., the Finite Element Method [1, 41, 33], Fourier transforms [39, 40, 13], or Stochastic Methods [34].

The fundamental limit of all “*homogenization methods*” approaches is the impossibility of adapting them to study composites with little regularity. In these cases, the different phases are typically modeled separately, as a continuum. This approach began with Pipkin [45] on two dimensional membranes, and was then expanded to three dimensional examples by others (see, e.g., [31] for a detailed bibliography).

Fully resolved methods allow richer structures, but require a high numerical resolution, especially when material phases have different scales. The complex meshing and coupling often result in an unbearable computational cost, limiting the use of these methods.

The purpose of this paper is to introduce a new approach which is fit for materials that have *intermediate* properties, i.e., they posses no particular regularity, and are made by a relatively high number of fiber components. We propose an FRMs model inspired by the Immersed Boundary Method (IBM) [43], and by its variational counterparts [10, 21, 23, 47, 24], where the elastic matrix and the fibers are modeled independently, and coupled through a non-slip condition. We aim at providing an efficient numerical method for FRMs that allows the modeling of complex networks of fibers, where one may also be interested in the elastic properties of single fibers, without requiring the resolution of the single fibers in the background elastic matrix. From the computational point of view, this approach allows the use of two independent discretizations: one describing the

fibers, and one describing the *whole domain*, i.e., both the elastic matrix and the fibers. A distributed Lagrange multiplier is used to couple the independent grids, following the same spirit of the finite element immersed boundary method [8, 10], separating the Cauchy stress of the whole material into a background uniform behavior and a *excess* elastic behavior on the fibers.

Section 2 introduces the classical fully resolved model of a collection of fibers immersed in an elastic matrix. For simplicity, we do not include dissipative terms, and restrict our study to linearly elastic materials. The problem is then reformulated exploiting classical results of mixed methods (see Chapter 4 of [7]), following ideas similar to those found in [9], proving that both the continuous and discrete formulations we propose are well-posed with a unique solution.

The use of a full three dimensional model for the fibers still results in high computational costs; the obvious simplification would be to approximate the fibers with one-dimensional structures. This approach is non-trivial because it is not possible to consider the restriction of a Sobolev function defined on a three-dimensional domain to a one-dimensional domain. A possible solution involves the use of weighted Sobolev spaces, combined with graded meshes [12, 11] but, if the number of fibers is large, graded meshes may still be too computationally intensive. In Section 3, we propose and analyze an alternative solution, where additional modellistic assumptions enable a $3D - 1D$ coupling that relies on local averaging techniques. A similar procedure is used in [22] to model vascularized tissues. To conclude, we validate our thin fiber model in Section 4, and draw some conclusions in Section 5.

2. Three-dimensional model

Many bi-phasic materials present a relatively simple fiber structure but result in a very intricate elastic matrix. Consider, for example, Figure 1: constructing a discretization grid for the fibers themselves maybe simple enough, but building a fully resolved grid for the *surrounding* elastic matrix, in this case, may require excessive resolution, and result in a computationally hard problem to solve. We wish to describe a new approach, where we substitute the complex mesh needed for the elastic matrix with a simple one describing the whole domain, and overlap the fiber structure independently with respect to the background grid, and couple the two systems via distributed Lagrange multipliers.

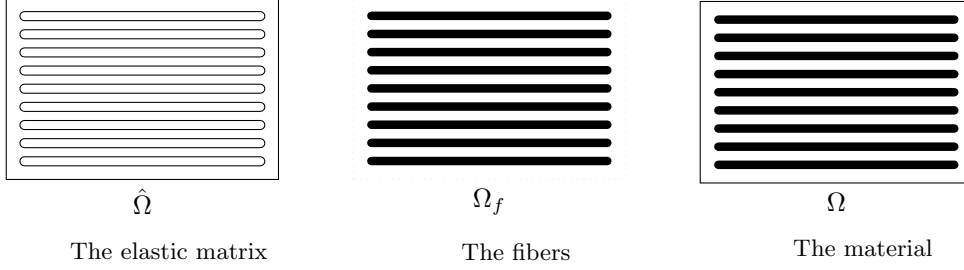
2.1. Problem formulation

As a model bi-phasic material, we consider a linearly elastic fiber reinforced material. To simplify the treatment of the problem, in this work we limit ourselves to the quasi-static small strain regime. The extension to finite strain elasticity and dynamic problems does not present additional difficulties and is going to be the subject of a future work.

To describe the composite, we use a connected, bounded, Lipschitz domain $\Omega \subset \mathbb{R}^d$ of dimension $d = 3$, composed of a fiber phase $\Omega_f \subset \Omega$, and an elastic matrix $\hat{\Omega} := \Omega \setminus \Omega_f \subset \mathbb{R}^d$, which we assume to be a connected, Lipschitz domain. We describe each of the $n_f \in \mathbb{N}$ fibers with a connected, Lipschitz domain and Ω_f is obtained as the union of these (possibly overlapping) domains.



Figure 1: An example of a fiber structure for which the mesh generation for the fibers would be trivial, but the resulting three-dimensional elastic matrix would be much more expensive to resolve in full.



Example of a two-dimensional section of an FRM with uniformly oriented fibers.

Remark. *The results of this section hold for a general domain Ω_f , union of multiple components with the required regularity. The property of the fibers of being thin, elongated, structures, is only needed for the model of Section 3, and plays no role in this Section.*

Given a displacement field $u: \Omega \rightarrow \mathbb{R}^d$, representing a deformation from the equilibrium configuration, the corresponding stress tensor on Ω can be expressed using the stress-strain law [15]:

$$S[u] = \mathbb{C} \nabla u,$$

where \mathbb{C} is a symmetric 4^{th} order tensor that takes the form:

$$\mathbb{C} = \begin{cases} \mathbb{C}_\Omega & \text{in } \hat{\Omega}, \\ \mathbb{C}_f & \text{in } \Omega_f. \end{cases} \quad (1)$$

Here \mathbb{C}_Ω and \mathbb{C}_f are assumed to be constant over their respective domains, and represent the elasticity tensors of the elastic matrix and of the fibers. The classical formulation of static linear elasticity can be thought of as a force balance equation (see, for example, [15]):

Problem 1 (Classic Strong Formulation). *Given an external force density field b , find the displacement u such that*

$$\begin{aligned} -\operatorname{div}(\mathbb{C}u) &= b && \text{in } \Omega, \\ u &= 0 && \text{on } \partial\Omega. \end{aligned} \quad (2)$$

Due to the piecewise nature of \mathbb{C} , it is natural to reformulate Problem 1 into a variational or weak formulation. We define the Sobolev space:

$$V := (H_{0,\partial\Omega}^1(\Omega))^d = \{v \in H^1(\Omega)^d : v|_{\partial\Omega} = 0\},$$

with norm $\|\cdot\|_V = \|\cdot\|_{H^1(\Omega)} := \|\cdot\|_\Omega + \|\nabla \cdot\|_\Omega$, where the symbol $\|\cdot\|_A$ represents the $L^2(A)$ norm over the measurable set $A \subset \Omega$, and $(\cdot, \cdot)_A$ represents the L^2 scalar product on the given domain A . The standard weak formulation reads:

Problem 2 (Classic Weak Formulation). *Given $b \in L^2(\Omega)^d$, find $u \in V$ such that:*

$$(\mathbb{C} \nabla u, \nabla v)_\Omega = (b, v)_\Omega \quad \forall v \in V. \quad (3)$$

The main idea behind our reformulation is to rewrite Problem 2 into an equivalent form, where we define two independent functional spaces. The novelty we introduce is to define the functional spaces on Ω and Ω_f , and not on $\hat{\Omega}$ and Ω_f . To achieve this, we define two fictitious materials: one with the same properties of the elastic matrix, occupying the full space Ω , and one describing the “excess elasticity” of the fibers separately, defined on Ω_f only. The first step in this direction is to split the left-hand side of Equation 3 on the two domains:

$$\begin{aligned} (\mathbb{C}\nabla u, \nabla v)_\Omega &= (\mathbb{C}_f \nabla u, \nabla v)_{\Omega_f} + (\mathbb{C}_\Omega \nabla u, \nabla v)_{\hat{\Omega}} \\ &= (\mathbb{C}_f \nabla u, \nabla v)_{\Omega_f} + \underbrace{(\mathbb{C}_\Omega \nabla u, \nabla v)_{\hat{\Omega}} + (\mathbb{C}_\Omega \nabla u, \nabla v)_{\Omega_f}}_{\Omega} - (\mathbb{C}_\Omega \nabla u, \nabla v)_{\Omega_f} \\ &= (\mathbb{C}_\Omega \nabla u, \nabla v)_\Omega + (\delta \mathbb{C}_f \nabla u, \nabla v)_{\Omega_f}, \end{aligned}$$

where $\delta \mathbb{C}_f := \mathbb{C}_f - (\mathbb{C}_\Omega)|_{\Omega_f}$.

For simplicity, we improperly use the expression “elastic matrix equation” and “fiber equation”, even though they should be really considered as the “whole domain equation”, and a “delta fiber equation”.

This formal separation does not change the original variational problem, which can still be stated explicitly: given $b \in L^2(\Omega)^d$, find $u \in V$ such that:

$$(\mathbb{C}_\Omega \nabla u, \nabla v)_\Omega + (\delta \mathbb{C}_f \nabla u, \nabla v)_{\Omega_f} = (b, v)_\Omega \quad \forall v \in V. \quad (4)$$

To simplify the coupling between the fibers and the elastic matrix, we need to split Equation 4 on two functional spaces, describing their boundary conditions.

The boundary of the domain Ω induces a natural splitting on the boundary of the fibers: we define the following partition of $\partial\Omega_f$:

$$B_i := \partial\Omega_f \setminus \partial\Omega \quad (5)$$

$$B_e := \partial\Omega \cap \partial\Omega_f, \quad (6)$$

where B_i is the interface between the fibers and the elastic matrix, while B_e is the interface between the fibers the exterior part of Ω , that lies on the boundary $\partial\Omega$.

Next we define the restriction of $H_0^1(\Omega)$ on the fibers:

$$W := V|_{\Omega_f} = (H_{0, B_e}^1(\Omega_f))^d. \quad (7)$$

With the explicit introduction of the space W we can modify Problem 2 by separating the solution into two components, one describing the whole matrix, the other describing the fibers. To couple the two parts we impose the following **non-slip** constraint for the solution $(u, w) \in V \times W$:

$$u|_{\Omega_f} = w. \quad (8)$$

The modified problem can be described as a constrained minimization problem:

$$u, w = \arg \inf_{\substack{u \in V \\ w \in W \\ \text{subject to} \\ u|_{\Omega_f} = w}} \psi(u, w), \quad (9)$$

where we defined the total elastic energy of the system as

$$\psi(u, w) = \frac{1}{2}(\mathbb{C}_\Omega \nabla u, \nabla u)_\Omega + \frac{1}{2}(\delta \mathbb{C}_f \nabla w, \nabla w)_{\Omega_f} - (b, u)_\Omega. \quad (10)$$

To impose the non-slip constraint of Equation 8 in weak form, several choices are possible. One may use, for example, the scalar product of W , or the duality product $W' \times W$ as in [9]. In this work, we choose the former: the H^1 scalar product in $Q := W$:

$$(q, u|_{\Omega_f} - w)_{H^1(\Omega_f)} = 0 \quad \forall q \in Q. \quad (11)$$

The constrained minimization expressed in Equation 9 is equivalent to the saddle point problem:

$$u, w, \lambda = \arg \inf_{\substack{u \in V \\ w \in W}} \left(\arg \sup_{\lambda \in Q} \psi(u, w, \lambda) \right), \quad (12)$$

where the constraint is imposed weakly as in 11 with a Lagrange multiplier:

$$\psi(u, w, \lambda) := \frac{1}{2}(\mathbb{C}_\Omega \nabla u, \nabla u)_\Omega + \frac{1}{2}(\delta \mathbb{C}_f \nabla w, \nabla w)_{\Omega_f} + (\lambda, u|_{\Omega_f} - w)_{H^1(\Omega_f)} - (b, u)_\Omega.$$

A solution to Equation 12 is obtained by solving the Euler-Lagrange equation:

$$\langle D_u \psi, v \rangle + \langle D_w \psi, y \rangle + \langle D_\lambda \psi, q \rangle = 0 \quad \forall v \in V, \forall y \in W, \forall q \in Q, \quad (13)$$

that is:

Problem 3 (Saddle Point Weak Formulation). *Given $b \in L^2(\Omega)^d$, find $u \in V, w \in W, \lambda \in Q$ such that:*

$$(\mathbb{C}_\Omega \nabla u, \nabla v)_\Omega + (\lambda, v|_{\Omega_f})_{H^1(\Omega_f)} = (b, v)_\Omega \quad \forall v \in V \quad (14)$$

$$(\delta \mathbb{C}_f \nabla w, \nabla y)_{\Omega_f} - (\lambda, y)_{H^1(\Omega_f)} = 0 \quad \forall y \in W \quad (15)$$

$$(q, u|_{\Omega_f} - w)_{H^1(\Omega_f)} = 0 \quad \forall q \in Q, \quad (16)$$

or, equivalently,

$$\begin{array}{llll} \mathcal{K}_\Omega u & + \mathcal{B}^T \lambda & = (b, \cdot)_\Omega & \text{in } V' \\ & \mathcal{K}_f w & - \mathcal{M}^T \lambda & = 0 & \text{in } W' \\ \mathcal{B} u & - \mathcal{M} w & & = 0 & \text{in } Q', \end{array} \quad (17)$$

where

$$\begin{array}{ll} \mathcal{K}_\Omega: V \rightarrow V' & \langle \mathcal{K}_\Omega u, \cdot \rangle := (\mathbb{C}_\Omega \nabla u, \nabla \cdot)_\Omega \\ \mathcal{K}_f: W \rightarrow W' & \langle \mathcal{K}_f w, \cdot \rangle := (\delta \mathbb{C}_f \nabla w, \nabla \cdot)_{\Omega_f} \\ \mathcal{B}: V \rightarrow Q' & \langle \mathcal{B} u, \cdot \rangle := (\cdot, u|_{\Omega_f})_{H^1(\Omega_f)} \\ \mathcal{M}: W \rightarrow Q' & \langle \mathcal{M} w, \cdot \rangle := (\cdot, w)_{H^1(\Omega_f)}. \end{array} \quad (18)$$

2.2. Well-posedness, existence and uniqueness

The theory for saddle point structure problems is well known and can be found, for example, in [7]. To verify well-posedness, existence and unicity of the solution to such a problem, it is sufficient for certain *inf* – *sup* and *ell* – *ker* conditions to be satisfied.

To make our notation closer to the one used in [7], we introduce the following Hilbert space, with its norm:

$$\begin{aligned}\mathbb{V} &:= V \times W, \\ \|(u, w)\|_{\mathbb{V}}^2 &:= \|u\|_V^2 + \|w\|_W^2.\end{aligned}$$

We indicate with $\mathbf{u} := (u, w)$, $\mathbf{v} := (v, y)$ the elements of \mathbb{V} , and define the following bilinear forms:

$$\begin{aligned}\mathbb{F}: \mathbb{V} \times \mathbb{V} &\longrightarrow \mathbb{R} \\ (\mathbf{u}, \mathbf{v}) &\longmapsto \langle \mathcal{K}_{\Omega} u, v \rangle + \langle \mathcal{K}_f w, y \rangle = (\mathbb{C}_{\Omega} \nabla u, \nabla v)_{\Omega} + (\delta \mathbb{C}_f \nabla w, \nabla y)_{\Omega_f}, \\ \mathbb{E}: \mathbb{V} \times Q &\longrightarrow \mathbb{R} \\ (\mathbf{u}, q) &\longmapsto \langle \mathcal{B} u, q \rangle - \langle \mathcal{M} w, q \rangle = (q, v|_{\Omega_f} - w)_{H^1(\Omega_f)}.\end{aligned}$$

Summing the first two equations of Problem 3 and using the newly defined space we can restate the problem as: find $\mathbf{u} \in \mathbb{V}$, $\lambda \in Q$ such that

$$\begin{aligned}\mathbb{F}(\mathbf{u}, \mathbf{v}) + \mathbb{E}^T(\lambda, \mathbf{v}) &= (b, v)_{\Omega} & \forall \mathbf{v} := (v, y) \in \mathbb{V}, \\ \mathbb{E}(\mathbf{u}, q) &= 0 & \forall q \in Q.\end{aligned}\tag{19}$$

Following [7], to state the *inf* – *sup* conditions we introduce the kernel

$$\begin{aligned}\ker \mathbb{E} &:= \left\{ \mathbf{v} := (v, w) \in \mathbb{V} : (q, v|_{\Omega_f} - w)_{H^1(\Omega_f)} = 0 \ \forall q \in Q \right\} \\ &= \left\{ \mathbf{v} := (v, w) \in \mathbb{V} : v|_{\Omega_f} = w \text{ a.e. on } \Omega_f \right\}.\end{aligned}$$

The problem is well-posed, and there exists a unique solution, if there exist two positive constants $\alpha_1 > 0$, $\alpha_2 > 0$ such that

$$\inf_{q \in Q} \sup_{\mathbf{v} \in \mathbb{V}} \frac{\mathbb{E}(\mathbf{u}, q)}{\|\mathbf{u}\|_{\mathbb{V}} \|q\|_Q} \geq \alpha_1 \tag{20}$$

$$\inf_{\mathbf{u} \in \ker \mathbb{E}} \sup_{\mathbf{v} \in \ker \mathbb{E}} \frac{\mathbb{F}(\mathbf{u}, \mathbf{v})}{\|\mathbf{u}\|_{\mathbb{V}} \|\mathbf{v}\|_{\mathbb{V}}} \geq \alpha_2. \tag{21}$$

These two conditions can be proved using the following Propositions:

Proposition 2.1. *There exists a constant $\alpha_1 > 0$ such that:*

$$\inf_{q \in Q} \sup_{(v, w) \in \mathbb{V}} \frac{(q, v|_{\Omega_f} - w)_{H^1(\Omega_f)}}{\|(v, w)\|_{\mathbb{V}} \|q\|_Q} \geq \alpha_1.$$

Proof. Using the definition of the norm in Q , for every $q \in Q$:

$$\begin{aligned} \|q\|_Q &= \sup_{w \in W} \frac{(q, w)_{H^1(\Omega_f)}}{\|w\|_W} = \sup_{w \in W} \frac{(q, -w)_{H^1(\Omega_f)}}{\|w\|_W} \\ &\leq \sup_{v \in V, w \in W} \frac{(q, v|_{\Omega_f} - w)_{H^1(\Omega_f)}}{(\|w\|_W^2 + \|v\|_V^2)^{\frac{1}{2}}}, \end{aligned}$$

where the last inequality can be proven fixing $v = 0$. The final statement is found dividing by $\|q\|_{\Omega_f}$ and taking the $\inf_{q \in Q}$. \square

Proposition 2.1 proves Inequality 20. To prove Inequality 21 additional hypotheses are needed:

Proposition 2.2. *Assume \mathbb{C}_Ω and \mathbb{C}_f to be strongly elliptical, with constants c_Ω and c_f respectively such that $c_f > c_\Omega > 0$; there exists a constant $\alpha_2 > 0$ such that:*

$$\inf_{(u, w) \in \ker \mathbb{E}} \sup_{(v, y) \in \ker \mathbb{E}} \frac{(\mathbb{C}_\Omega \nabla u, \nabla v)_\Omega + (\delta \mathbb{C}_f \nabla w, \nabla y)_{\Omega_f}}{\|(v, y)\|_V \|(u, w)\|_V} \geq \alpha_2.$$

Proof. Using the hypotheses we can easily prove that $\delta \mathbb{C}_f$ is elliptic of constant $c_f - c_\Omega$. For every $(u, w) \in \ker(\mathbb{E})$:

$$\begin{aligned} \sup_{(v, y) \in \ker(\mathbb{E})} \frac{(\mathbb{C}_\Omega \nabla u, \nabla v)_\Omega + (\delta \mathbb{C}_f \nabla w, \nabla y)_{\Omega_f}}{\|(v, y)\|_V} &\geq \frac{c_\Omega(u, u)_{H^1(\Omega)} + (c_f - c_\Omega)(w, w)_{H^1(\Omega_f)}}{\|(u, w)\|_V} \\ &\geq \alpha_2 \|(u, w)\|_V. \end{aligned}$$

Where we used the H^1 scalar product on Ω : $H^1(\Omega) := (u, v)_\Omega + (\nabla u, \nabla v)_\Omega$.

The result is obtained dividing by $\|(u, w)\|_V$ and considering the $\inf_{(u, w) \in \ker \mathbb{E}}$. \square

Remark. *This paper does not intend to focus on the choice of elastic tensors. Strong ellipticity is a common property among them, and holds in the case of linearly elastic materials (see e.g. [37]): let $u \in V$, $w \in W$*

$$\mathbb{C}_\Omega \nabla u := 2\mu_\Omega Eu + \lambda_\Omega (\text{tr} \nabla u) I = 2\mu_\Omega Eu + \lambda_\Omega (\text{div } u) I \quad (22)$$

$$\mathbb{C}_f \nabla w := 2\mu_f Ew + \lambda_f (\text{tr} \nabla w) I = 2\mu_f Ew + \lambda_f (\text{div } w) I \quad (23)$$

$$\begin{aligned} \delta \mathbb{C}_f \nabla w &:= 2(\mu_f - \mu_\Omega) Ew + (\lambda_f - \lambda_\Omega) (\text{tr} \nabla w) I \\ &= 2\mu_\delta Ew + \lambda_\delta (\text{div } w) I, \end{aligned} \quad (24)$$

where $\mu_\delta := \mu_f - \mu_\Omega$ and $\lambda_\delta := \lambda_f - \lambda_\Omega$. These are the elastic tensors we shall use in Section 4, for our numerical tests.

Proposition 2.2 implies Inequality 21, and we conclude that Problem 3 is well-posed, and has a unique solution.

2.3. Finite element discretization

The formulation of Problem 3 makes it possible to consider independent, separate triangulations for its numerical solution. Consider the family $\mathcal{T}_h(\Omega)$ of regular meshes in Ω , and a family $\mathcal{T}_h(\Omega_f)$ of regular meshes in Ω_f , where we denote by h the maximum diameter of the elements of the two triangulations. We assume that no geometrical error is committed when meshing, i.e., $\Omega = \bigcup_{T_h \in \mathcal{T}_h(\Omega)} T_h$, and $\Omega_f = \bigcup_{S_h \in \mathcal{T}_h(\Omega_f)} S_h$. We consider two independent finite element spaces $V_h \subset V$, and $W_h \subset W$. The natural choice for Q_h is to use the same space used for the discretisation of W_h . By hypothesis, for every $v_h \in V_h$, $v_h|_{\Omega_f} \in W$; however, the meshes are taken to be independent and non-matching, and we do not know *a priori* if $v_h|_{\Omega_f} \in W_h$. Using the equivalence of norms in a finite space, we describe the non-slip condition utilizing the L^2 scalar product on Ω_f .

To handle the restriction of functions from V_h to W_h , we introduce the L^2 projection:

$$P_W: L^2(\Omega_f) \rightarrow W_h \subset L^2(\Omega_f),$$

which is continuous: for every $u \in L^2(\Omega_f)$

$$\|P_W u\|_{L^2(\Omega_f)} \leq \|u\|_{L^2(\Omega_f)}.$$

This condition is too weak for our Problem, which involves ∇w . We make the further assumption that the restriction $P_W|_W \neq 0$, and is H^1 -stable, i.e., there exists a positive constant c , such that for all $w \in W$:

$$\|\nabla P_W|_W w\|_{\Omega_f} \leq c \|\nabla w\|_{\Omega_f}. \quad (25)$$

With a slight abuse of notation we use P_W instead of $P_W|_W$. We assume that this stability property holds uniformly on $\mathcal{T}_h(\Omega)$ and $\mathcal{T}_h(\Omega_f)$, provided that the mesh size h is comparable on the two domains. A proof of the H^1 -stability is available in [14] for a particular choice of discretization spaces. A general result for all non-matching grids is still not available.

To discretize Problem 3, we first reformulate the weak non-slip condition 11: for every $v_h \in V_h, w_h \in W_h, q_h \in Q_h$:

$$\begin{aligned} (q_h, v_h|_{\Omega_f} - w_h)_{\Omega_f} &= (q_h, v_h|_{\Omega_f})_{\Omega_f} - (q_h, w_h)_{\Omega_f} \\ &= (q_h, P_W v_h)_{\Omega_f} - (q_h, w_h)_{\Omega_f} = (q_h, P_W v_h - w_h)_{\Omega_f}. \end{aligned}$$

Problem 4 (Discrete Weak Formulation). *Given $b \in L^2(\Omega)^d$, find $u_h \in V_h, w_h \in W_h, \lambda_f \in Q_h$ such that:*

$$(\mathbb{C}_\Omega \nabla u_h, \nabla v_h)_\Omega + (\lambda_h, P_W v_h)_{\Omega_f} = (b, v_h)_\Omega \quad \forall v_h \in V_h, \quad (26)$$

$$(\delta \mathbb{C}_f \nabla w_h, \nabla y_h)_{\Omega_f} - (\lambda_h, y_h)_{\Omega_f} = 0 \quad \forall y_h \in W_h, \quad (27)$$

$$(q_h, P_W u_h - w_h)_{\Omega_f} = 0 \quad \forall q_h \in Q_h. \quad (28)$$

As in the continuous case, we study the *inf - sup* conditions after defining the following space:

$$\mathbb{V}_h := V_h \times W_h,$$

equipped with the norm $\|\cdot\|_{\mathbb{V}}$, and the operators:

$$\begin{aligned}\mathbb{F}_h &: \mathbb{V}_h \times \mathbb{V}_h \longrightarrow \mathbb{R} \\ (\mathbf{u}_h, \mathbf{v}_h) &\longmapsto (\mathbb{C}_\Omega \nabla u_h, \nabla v_h)_\Omega + (\delta \mathbb{C}_f \nabla w_h, \nabla y_h)_{\Omega_f}, \\ \mathbb{E}_h &: \mathbb{V}_h \times Q_h \longrightarrow \mathbb{R} \\ (\mathbf{u}_h, q_h) &\longmapsto (q_h, P_W v_h - w_h)_{\Omega_f}.\end{aligned}$$

Equation 19 can now be discretized: find $\mathbf{u}_h \in \mathbb{V}_h, \lambda_h \in Q_h$ such that

$$\begin{aligned}\mathbb{F}_h(\mathbf{u}_h, \mathbf{v}_h) + \mathbb{E}_h^T(\lambda_h, \mathbf{v}_h) &= (b, v_h)_\Omega, & \forall \mathbf{v}_h := (v_h, y_h) \in \mathbb{V}_h \\ \mathbb{E}_h(\mathbf{u}_h, q_h) &= 0 & \forall q_h \in Q_h.\end{aligned}$$

Following Subsection 2.2, Problem 4 is well-posed, and there exists a unique solution if there exist two positive constants $\alpha_3 > 0, \alpha_4 > 0$ such that

$$\begin{aligned}\inf_{q_h \in Q_h} \sup_{\mathbf{v}_h \in \mathbb{V}_h} \frac{\mathbb{E}(\mathbf{u}_h, q_h)}{\|\mathbf{u}_h\|_{\mathbb{V}} \|q_h\|_{\Omega_f}} &\geq \alpha_3 \\ \inf_{\mathbf{u}_h \in \ker \mathbb{E}_h} \sup_{\mathbf{v}_h \in \ker \mathbb{E}_h} \frac{\mathbb{F}(\mathbf{u}_h, \mathbf{v}_h)}{\|\mathbf{u}_h\|_{\mathbb{V}_h} \|\mathbf{v}_h\|_{\mathbb{V}_h}} &\geq \alpha_4.\end{aligned}$$

These conditions can be proved modifying Propositions 2.1 and 2.2:

Proposition 2.3. *There exists a constant $\alpha_3 > 0$, independent of h , such that:*

$$\inf_{q_h \in Q_h} \sup_{(v_h, w_h) \in \mathbb{V}_h} \frac{(q_h, P_W v_h - w_h)_{\Omega_f}}{\|(v_h, w_h)\|_{\mathbb{V}} \|q_h\|_{\Omega_f}} \geq \alpha_3.$$

Proof. In finite dimensional spaces norms are equivalent: there exists a C_H such that $\|w_h\|_W \leq C_H \|w_h\|_{\Omega_f}$ for every $w_h \in W_h$.

Using the definition of the norm in Q_h , and the fact that it is the same space of W_h with a different norm, for every $q_h \in Q_h$:

$$\begin{aligned}\|q_h\|_{\Omega_f} &= \sup_{w_h \in W_h} \frac{(q_h, w_h)_{\Omega_f}}{\|w_h\|_{\Omega_f}} = \sup_{w_h \in W_h} \frac{(q_h, -w_h)_{\Omega_f}}{\|w_h\|_{\Omega_f}} \\ &\leq C_H \sup_{w_h \in W_h} \frac{(q_h, -w_h)_{\Omega_f}}{\|w_h\|_W} \leq C_H \sup_{w_h \in W_h, v_h \in V_h} \frac{(q_h, P_W v_h - w_h)_{\Omega_f}}{(\|w_h\|_W^2 + \|v_h\|_V^2)^{\frac{1}{2}}},\end{aligned}$$

and we conclude as in Proposition 2.1. \square

To study the *ell* – *ker* condition on \mathbb{F}_h we define:

$$\begin{aligned}\ker(\mathbb{E}_h) &:= \{\mathbf{v}_h := (v_h, w_h) \in \mathbb{V}_h : (q_h, P_W v_h - w_h)_{\Omega_f} = 0 \quad \forall q_h \in Q_h\} \\ &= \{\mathbf{v}_h := (v_h, w_h) \in \mathbb{V}_h : (q_h, P_W v_h)_{\Omega_f} = (q_h, w_h)_{\Omega_f} \quad \forall q_h \in Q_h\}.\end{aligned}$$

Proposition 2.4. Assume \mathbb{C}_Ω and \mathbb{C}_f to be strongly elliptical with constants c_Ω and c_f respectively such that $c_\Omega > c_f > 0$; there exists a constant $\alpha_4 > 0$, independent of h , such that:

$$\inf_{(u_h, w_h) \in \ker(\mathbb{E})_h} \sup_{(v_h, y_h) \in \ker(\mathbb{E})_h} \frac{(\mathbb{C}_\Omega \nabla v_h, \nabla u_h)_\Omega + (\delta \mathbb{C}_f \nabla y_h, \nabla w_h)_{\Omega_f}}{\|(v_h, y_h)\|_V \|(u_h, w_h)\|_V} \geq \alpha_4.$$

Proof. *Mutatis mutandis*, the proof follows the one of Proposition 2.2. \square

Error estimate. Proposition 2.1 and 2.2 allow us to apply Theorem 5.2.5 of [7], obtaining the following error estimate:

Theorem 2.1. Consider \mathbb{C}_Ω and \mathbb{C}_f , elastic stress tensors satisfying the hypothesis of Proposition 2.2, the domains Ω and Ω_f with the regularity required in Section 2, and $b \in L^2(\Omega)^d$. Then the following error estimate holds for (u, w) , solution of Problem 3, and (u_h, w_h) , solution of Problem 4:

$$\|u - u_h\|_V + \|w - w_h\|_V \leq C_e \left(\inf_{v_h \in V_h} \|u - v_h\| + \inf_{y_h \in W_h} \|w - y_h\| \right), \quad (29)$$

where $C_e > 0$, and depends on $\alpha_3, \alpha_4, c_\Omega, c_f$ and the norm of the operators $\|\mathcal{K}_\Omega + \mathcal{K}_f\|$.

We remark how this constant C_e depends on α_3 , which is affected by the coupling between the two meshes. As intuition suggests, the quality of the solution does not depend only on the ability of V and W to individually describe it, but also on the coupling between them.

Non-matching meshes. One of the basic assumptions made in the continuous case is the inclusion:

$$W \subseteq V.$$

With an independent discretization of the two meshes the inclusion $W_h \subset V_h$ can not be guaranteed, leading to the use of the projection $P_W: V_h \rightarrow W_h$, which we require to be H^1 -stable i.e. that Equation 25 holds.

Since for every $\mathbf{v} = (v, w) \in \ker(\mathbb{E}_h) \Rightarrow P_W(v) = w \Rightarrow w \in P_W(V_h)$; if the set $P_W(V_h)$ is small, the *inf* – *sup* constant can be negatively affected; the extreme case being $P_W = 0$, which results in $\ker(\mathbb{E}_h) = \{(0, 0)\}$, and the *inf* – *sup* condition for \mathbb{F}_h not satisfied.

Under some simple construction hypotheses it is possible to guarantee that globally constant and linear functions are included in the kernel, so that $\ker(\mathbb{E}) \neq \{(0, 0)\}$. This is sufficient for the *inf* – *sup* condition to hold, but the constant α_3 might become very small, affecting the constant C_e used for Inequality 29, and resulting in a high error for the method.

3. Thin fibers

The computational cost of discretizing explicitly numerous three-dimensional fibers might render Problem 4 too computationally intensive: a possible simplification is suggested by the fiber shape, which can be approximated with a one-dimensional structure.

Constructing this simplified model is a non-trivial task because the restriction (or trace) of a three-dimensional function to a one-dimensional domain is not well defined in Sobolev spaces.

Instead of resorting to weighted Sobolev spaces and graded meshes, as done in [12, 11], the solution we propose is to introduce additional modellistic hypotheses, that allow one to use averaging techniques instead of traces to render the problem well posed.

To simplify the exposition, we shall consider a single fiber; the same results hold with a finite collection of fibers.

We begin introducing some definitions: let Γ be a one-dimensional connected domain, embedded in Ω , let $I \subset \mathbb{R}$ be a finite interval and $X: I \rightarrow \Gamma$ be a parametrization of Γ . We assume the Frenet trihedron $(\mathbf{t}(s), \mathbf{n}(s), \mathbf{b}(s))$ to be well defined for every $s \in I$, at every point $X(s) \in \Gamma$, and the function $s \mapsto (\mathbf{t}(s), \mathbf{n}(s), \mathbf{b}(s))$ to be continuous. Sufficient conditions to satisfy these hypotheses are well-known in literature, e.g., using a regular smooth curve.

Given a constant radius $a \in \mathbb{R}$, $a > 0$, the physical fiber Ω_a is described by a tubular neighbourhood of Γ :

$$\Omega_a := \{X(s) + \mathbf{n}(s)\lambda_1 + \mathbf{b}(s)\lambda_2 : s \in I; \lambda_1, \lambda_2 \in \mathbb{R} \text{ s.t. } \sqrt{\lambda_1^2 + \lambda_2^2} \leq a\}, \quad (30)$$

where we assume $\Omega_a \subset \Omega$. For all $x \in \Gamma$, we define $D_a(x)$ as the two-dimensional disk perpendicular to Γ , with radius a , centered at x :

$$D_a(x) := \{x + \mathbf{n}(s)\lambda_1 + \mathbf{b}(s)\lambda_2 : \lambda_1, \lambda_2 \in \mathbb{R}, \sqrt{\lambda_1^2 + \lambda_2^2} \leq a\}.$$

Remark. Under the previous hypotheses, there exists a diffeomorphism Φ of Ω to another domain Θ , such that $\Phi(\Omega_a)$ is a cylinder of radius a , with Γ transformed in a straight segment, the cylinder's axis. To avoid a heavy notation, requiring multiple uses of Φ and Φ^{-1} , we prove our results on $\Phi(\Omega_a)$, with coordinates (x, y, z) , where x is aligned with the fiber direction.

We now modify the definitions of Section 2, for the boundaries of $\partial\Omega_a$:

$$\begin{aligned} B_i &:= \partial\Omega_a \setminus \partial\Omega, \\ B_e &:= \partial\Omega \cap \partial\Omega_a, \\ V &:= (H_{0,\partial\Omega}^1(\Omega))^d, \\ W &:= (H_{0,\partial\Omega}^1(\Omega))^d \Big|_{\Omega_a}, \end{aligned}$$

with $d = 3$.

As a reference model, we consider small deformations of an FRM in which fibers are stiff compared to the underlying matrix. For this model, the fiber radius can be considered to be approximately constant:

First modellistic hypothesis: fixed radius. We assume the fiber's radius a to remain constant. This implies that the fiber displacement w is an element of \hat{W} , where:

$$\hat{W} := \{w \in W : \text{for a.e. } x \in \Gamma, w|_{D_a(x)} \equiv w(x) \text{ a.e. on } D_a(x)\}. \quad (31)$$

It is useful to introduce the space of functions of V which, restricted to Ω_a , belong to \hat{W} :

$$\hat{V} := \{v \in V : v|_{\Omega_a} \in \hat{W}\}.$$

Given $\hat{w} \in \hat{W}$, Equation 31 suggests to define the one-dimensional function $x \rightarrow w(x) = \hat{w}(x, 0, 0)$ for a. e. $x \in \Gamma$; a consequence of the absolutely continuous characterization of Sobolev functions[16] is that $\hat{w} \in H_{0,B_e}^1(\Gamma)$. This suggests the following definition:

$$W_\Gamma := (H_{0,B_e}^1(\Gamma))^d. \quad (32)$$

Notice that \hat{W} is isomorphic to $(W_{0,B_e}^{1,1}(\Gamma))^d$, and W_Γ is dense in $(W_{0,B_e}^{1,1}(\Gamma))^d$: as an additional hypothesis we assume the solution can be represented by a one-dimensional element $w \in W_\Gamma$.

Since $w \in \hat{W}$ is constant over every disk $D_a(x)$, so is the gradient ∇w : the elastic stress can be computed using only the values along Γ :

$$\frac{1}{2}(\delta \mathbb{C}_f \nabla w, \nabla w)_a = c_\Gamma (\delta \mathbb{C}_f \nabla w, \nabla w)_\Gamma, \quad (33)$$

with $c_\Gamma := \frac{\pi a^2}{2}$.

Second modellistic hypothesis: average non-slip condition. Let $u \in V$, we define the following function for a.e. $x \in \Gamma$:

$$\bar{u}(x) := \frac{1}{|D_a(0)|} \int_{D_a(x)} u(y) dD_y, \quad (34)$$

with $\bar{u} \in W_\Gamma$ (for the technical proof see Appendix A), and the following **average non-slip** condition can be formulated:

$$\bar{u} = w. \quad (35)$$

When considering $w \in \hat{W}, u \in \hat{V}$, the classic non-slip condition, described in Equation 8, is equivalent to Equation 35. As a second modellistic hypothesis we assume that the average non-slip condition can replace the non-slip condition.

3.1. Problem formulation

We assume the Modellistic Hypotheses described in the previous section hold:

- the fiber displacement w is described as an extension of W_Γ to an element of \hat{W} ,
- we can impose the coupling between fibers and elastic matrix through the average non-slip condition .

This allows us to modify Problem 3 for the $3D - 1D$ case; the weak formulation of the average non-slip constraint on Γ is:

$$(q, \bar{u} - w)_{H^1(\Gamma)} = 0 \quad \forall q \in Q_\Gamma,$$

with $Q_\Gamma := H^1(\Gamma)^d$.

For every $(u, w, q) \in V \times W_\Gamma \times Q_\Gamma$, we define the energy functional of our problem as:

$$\psi_T(u, w, \lambda) = \frac{1}{2}(\mathbb{C}_\Omega \nabla u, \nabla u)_\Omega + c_\Gamma(\delta \mathbb{C}_f \nabla w, \nabla w)_\Gamma + (q, \bar{u} - w)_{H^1(\Gamma)} - (b, u)_\Omega.$$

Then the saddle point problem becomes:

$$u, w, \lambda = \arg \inf_{\substack{u \in V \\ w \in W_\Gamma}} \left(\arg \sup_{\lambda \in Q_\Gamma} \psi_T(u, w, \lambda) \right). \quad (36)$$

Using the Euler-Lagrange equations as in Section 2.1, we obtain:

Problem 5 (1D-3D Weak Formulation). *Given $b \in L^2(\Omega)^d$, find $u \in V, w \in W_\Gamma, \lambda \in Q_\Gamma$ such that:*

$$\begin{aligned} (\mathbb{C}_\Omega \nabla u, \nabla v)_\Omega + (\lambda, \bar{v})_{H^1(\Gamma)} &= (b, v)_\Omega & \forall v \in V, \\ c_\Gamma(\delta \mathbb{C}_f \nabla w, \nabla y)_\Gamma - (\lambda, y)_{H^1(\Gamma)} &= 0 & \forall y \in W_\Gamma, \\ (q, \bar{u} - w)_{H^1(\Gamma)} &= 0 & \forall q \in Q_\Gamma. \end{aligned}$$

We now re-define the space $\mathbb{V} := V \times W_\Gamma$, and its norm: for every $(v, y) \in \mathbb{V}$, $\|(v, y)\|_{\mathbb{V}} := \|\cdot\|_V + \|\cdot\|_{W_\Gamma}$. We define the operators for the tubular fiber Ω_a :

$$\begin{aligned} \mathbb{F}_T &:= (\mathbb{C}_\Omega \nabla u, \nabla v)_\Omega + c_\Gamma(\delta \mathbb{C}_f \nabla w, \nabla w)_\Gamma, \\ \mathbb{E}_T &:= (q, \bar{u} - w)_{H^1(\Gamma)}, \end{aligned}$$

obtaining a new saddle-point problem, which we study using the *inf* – *sup* conditions.

3.2. Well-posedness, existence and uniqueness

Proposition 3.1. *There exists a constant $\alpha_5 > 0$ such that:*

$$\inf_{q \in Q_\Gamma} \sup_{(v, w) \in \mathbb{V}} \frac{(q, \bar{v} - w)_{H^1(\Gamma)}}{\|(v, w)\|_{\mathbb{V}} \|q\|_Q} \geq \alpha_5.$$

Proof. Using the definition of the norm in Q_Γ , and the density of W_Γ in Q_Γ , for every $q \in Q_\Gamma$:

$$\begin{aligned} \|q\|_{H^1(\Gamma)} &= \sup_{y \in Q_\Gamma} \frac{(q, y)_{H^1(\Gamma)}}{\|y\|_Q} = \sup_{w \in W_\Gamma} \frac{(q, w)_{H^1(\Gamma)}}{\|w\|_W} \\ &= \sup_{w \in W_\Gamma} \frac{(q, -w)_{H^1(\Gamma)}}{\|w\|_W} \leq \sup_{v \in \hat{V}, w \in W_\Gamma} \frac{(q, \bar{v} - w)_{H^1(\Gamma)}}{(\|w\|_W^2 + \|v\|_V^2)^{1/2}}, \end{aligned}$$

where the last inequality can be proven fixing $v = 0$. We conclude in a similar manner to Proposition 2.2. \square

Define the kernel of \mathbb{E}_T :

$$\ker \mathbb{E}_T := \{\mathbf{u} = (u, w) \in \mathbb{V} : (q, \bar{u} - w)_{H^1(\Gamma)} = 0 \quad \forall q \in Q_\Gamma\}.$$

Proposition 3.2. Assume \mathbb{C}_Ω and \mathbb{C}_f to be strongly elliptical, with constants c_Ω and c_f respectively such that $c_\Omega > c_f > 0$; there exists a constant $\alpha_6 > 0$ such that:

$$\inf_{(u,w) \in \ker \mathbb{E}_T} \sup_{(v,y) \in \ker \mathbb{E}_T} \frac{(\mathbb{C}_\Omega \nabla v, \nabla u)_\Omega + c_\Gamma (\delta \mathbb{C}_f \nabla y, \nabla w)_\Gamma}{\|(v,y)\|_{\mathbb{V}} \|(u,w)\|_{\mathbb{V}}} \geq \alpha_6.$$

Proof. For every $(u,w) \in \ker(\mathbb{E}_h)$:

$$\begin{aligned} \sup_{(v,y) \in \ker(\mathbb{E})} \frac{(\mathbb{C}_\Omega \nabla u, \nabla v)_\Omega + (\delta \mathbb{C}_f \nabla w, \nabla y)_\Gamma}{\|(v,y)\|_{\mathbb{V}}} &\geq \frac{c_\Omega(u,u)_{H^1(\Omega)} + (c_f - c_\Omega)(w,w)_{H^1(\Gamma)}}{\|(u,w)\|_{\mathbb{V}}} \\ &\geq \alpha_6 \|(u,w)\|_{\mathbb{V}}. \end{aligned}$$

The result is obtained dividing and considering the $\inf_{(u,w) \in \ker \mathbb{E}_T}$.

□

Using the saddle point theory we conclude that, under our modellistic assumptions, Problem 5 is well-posed, and has a unique solution.

3.3. Finite element discretization

The discretization of Problem 5 for thin fibers follows the steps of Section 2.3, on the domains Ω and Γ (the fiber's one-dimensional core). Consider two independent discretizations for these domains; the family $\mathcal{T}_h(\Omega)$ of regular meshes in Ω , and a family $\mathcal{T}_h(\Gamma)$ of regular meshes in Γ . We assume no geometrical error is committed when meshing.

We consider two independent finite element discretizations $V_h \subset V$, $W_h \subset W_\Gamma$ and define the space Q_h as the space W_h . Utilizing the norm equivalence, we describe the non-slip condition using the $L^2(\Gamma)$ scalar product. We can now write the discretization of Problem 5:

Problem 6 (1D-3D Discretized Weak Formulation). *Given $b \in L^2(\Omega)^d$, find $u_h \in V_h, w_h \in W_h, \lambda_h \in Q_h$ such that:*

$$(\mathbb{C}_\Omega \nabla u_h, \nabla v_h)_\Omega + (\lambda_h, \bar{v}_h)_\Gamma = (b, v_h)_\Omega \quad \forall v_h \in V_h, \quad (37)$$

$$c_\Gamma (\delta \mathbb{C}_f \nabla w_h, \nabla y_h)_\Gamma - (\lambda_h, y_h)_\Gamma = 0 \quad \forall y_h \in W_h, \quad (38)$$

$$(q_h, \bar{u}_h - w_h)_\Gamma = 0 \quad \forall q_h \in Q_h. \quad (39)$$

To study the saddle-point problem we define the Hilbert space $\mathbb{V}_h := V_h \times W_h$, with its norm, and the operators

$$\begin{aligned} \mathbb{F}_{T,h}: \mathbb{V}_h \times \mathbb{V}_h &\longrightarrow \mathbb{R} \\ (\mathbf{u}_h, \mathbf{v}_h) &\longmapsto (\mathbb{C}_\Omega \nabla u_h, \nabla v_h)_\Omega + (\delta \mathbb{C}_f \nabla w_h, \nabla y_h)_\Gamma, \\ \mathbb{E}_{T,h}: \mathbb{V}_h \times Q_h &\longrightarrow \mathbb{R} \\ (\mathbf{u}_h, q_h) &\longmapsto (q_h, \bar{u}_h - w_h)_\Gamma. \end{aligned}$$

Then we can rewrite problem 6 in operatorial form, showing its saddle-point structure: find $\mathbf{u}_h \in \mathbb{V}_h, \lambda_h \in Q_h$ such that:

$$\begin{aligned}\mathbb{F}_{T,h}(\mathbf{u}_h, \mathbf{v}_h) + \mathbb{E}_{T,h}^T(\lambda_h, \mathbf{v}_h) &= (b_h, v_h)_\Omega & \forall \mathbf{v}_h := (v_h, y_h) \in \mathbb{V}_h \\ \mathbb{E}_{T,h}(q_h, \mathbf{u}_h) &= 0 & \forall q_h \in Q_h.\end{aligned}$$

Since standard finite element functions are continuous, it is possible to directly consider their restriction to Γ . Define the L^2 projection $P_{W_\Gamma}: L^2(\Gamma) \rightarrow W_h \subset L^2(\Gamma)$. By hypothesis, for every $u_h \in L^2(\Gamma)$:

$$\|P_{W_\Gamma} u\|_{L^2(\Gamma)} \leq \|u\|_{L^2(\Gamma)}.$$

Consider now the restriction $P_{W_\Gamma}|_{W_\Gamma}$ (with a slight abuse of notation we call it P_{W_Γ}); we make the additional assumption that P_{W_Γ} is H^1 -stable, that is there exists a positive constant c , such that for all $w \in W_\Gamma$:

$$\|\nabla P_{W_\Gamma} w_h\|_{L^2(\Gamma)} \leq c \|\nabla w_h\|_{L^2(\Gamma)}. \quad (40)$$

If we are considering a family of triangulations, then let c be a constant such that the last inequality holds true for all considered triangulations.

Proposition 3.3. *There exists a constant $\alpha_7 > 0$, independent of h , such that:*

$$\inf_{q_h \in W_h} \sup_{(v_h, w_h) \in \mathbb{V}_h} \frac{(q_h, \bar{v}_h - w_h)_\Gamma}{\|(v_h, w_h)\|_{\mathbb{V}} \|q_h\|_\Gamma} \geq \alpha_7.$$

Proof. This is a variation on the proof of Proposition 3.1.

In finite dimensional spaces norms are equivalent: that there exists a C_H such that $\|w_h\|_W \leq C_H \|w_h\|_{\Omega_f}$ for every $w_h \in W_h$. Using the definition of the norm in Q_h , the fact that it is the same space of W_h with a different norm, for every $q_h \in Q_h$:

$$\begin{aligned}\|q_h\|_\Gamma &= \sup_{w_h \in W_h} \frac{(q_h, w_h)_\Gamma}{\|w_h\|_\Gamma} \leq C_H \sup_{w_h \in W_h} \frac{(q_h, w_h)_\Gamma}{\|w_h\|_W} \\ &\leq C_H \sup_{v_h \in V_h, w_h \in W_h} \frac{(q_h, v_h|_W - w_h)_\Gamma}{(\|w_h\|_W^2 + \|v_h\|_V^2)},\end{aligned}$$

we conclude as in Proposition 2.1. \square

To study the inf-sup condition for $\mathbb{F}_{T,h}$ define:

$$\begin{aligned}\ker(\mathbb{E}_{T,h}) &:= \{\mathbf{v}_h \in \mathbb{V}_h : (q_h, \bar{v}_h - w_h)_\Gamma = 0 \quad \forall q_h \in Q_h\} \\ &= \{\mathbf{v} \in \mathbb{V}_h : (q_h, \bar{v}_h)_\Gamma = (q_h, w_h)_\Gamma \quad \forall q_h \in Q_h\}.\end{aligned}$$

Proposition 3.4. *Assume \mathbb{C}_Ω and \mathbb{C}_f to be strongly elliptical, with constants c_Ω and c_f respectively such that $c_\Omega > c_f > 0$; then there exists a constant $\alpha_8 > 0$, independent of h , such that:*

$$\inf_{(u_h, w_h) \in \ker(\mathbb{E}_{T,h})} \sup_{(v_h, y_h) \in \ker(\mathbb{E}_{T,h})} \frac{(\mathbb{C}_\Omega \nabla v_h, \nabla u_h)_\Omega + (\delta \mathbb{C}_f \nabla y_h, \nabla w_h)_\Gamma}{\|(v_h, y_h)\|_{\mathbb{V}} \|(u_h, w_h)\|_{\mathbb{V}}} \geq \alpha_8.$$

Proof. The proof is almost identical to the one of proposition 3.2. \square

One-Dimensional Approximation. The approach of Section 3 hides a computational difficulty: given $v_h \in V_h$, the average \bar{v}_h is obtained computing a number of two-dimensional integrals, nullifying the computational advantage of using one-dimensional fibers.

Since we are using finite element functions, there is a straight-forward solution to this problem: approximate \bar{v}_h with the restriction $v_h|_\Gamma$. This approximation is exact for every $v_h \in \hat{V}$, and can be justified by the fact that for every $v_h \in V_h$:

$$\lim_{a \rightarrow 0} \bar{v}_h(x) = v_h(x) \quad \text{for every } x \in \Gamma,$$

coherently with the initial choice of \bar{v}_h as a “substitute” of v_h .

While this approach simplifies our computations, it makes difficult the derivation of a formula for the error committed. The theoretical basis for such an estimate have been described in this paper, the estimate itself shall be the subject of future work.

4. Numerical validation

The analytical solution of Problems 3 and 5, even for simple configurations, is non-trivial: we chose some FRMs structures which are studied in literature, and used the known approximated solutions as a comparison for our model.

Using the deal.II library [3, 4, 35, 48], and the deal.II step-60 tutorial [32] we developed a model for thin fibers proposed in Section 3, and compared it with the Rule of Mixtures and the Halpin-Tsai configurations in some pull/push tests.

Numerical Setting. For our numerical solution, we now describe how to solve Problem 6 on a collection of fibers, while reducing the system size; we begin by redefining our spaces and meshes:

- Ω : the elastic matrix, on which we build the finite element space, of dimension $N \in \mathbb{N}$:

$$V_h = \text{span}\{v_i\}_{i=1}^N \subset H^1(\Omega).$$

- $\Gamma \subset \Omega$: the collection of $n_f \in \mathbb{N}$ fibers, i.e., $\Gamma := \bigcup_{k=1}^{n_f} \Gamma_k$, with the finite element discretization, of dimension $M \in \mathbb{N}$:

$$W_h = \text{span}\{w_a\}_{a=1}^M \subset H^1(\Gamma).$$

- Q_h : the space of the Lagrange multiplier, discretized using the same base of W_h .

We use i, j as indices for the space V_h and a, b as indices for the space W_h , and assume all hypotheses on spaces and meshes of section 3.3 are satisfied.

We assume that each fiber is parametrized by $X_k: I_k \rightarrow \Gamma_k$, where I_k is a finite interval in \mathbb{R} , and $1 \leq k \leq n_f$. We assume for any $1 \leq j < k \leq n_f$ we have $I_k \cap I_j = \emptyset$. Then we can define $X: \bigcup_{k=1}^{n_f} I_k \rightarrow \Gamma$, which parametrizes all fibers contained in Γ . For each fiber Γ_k we define its tubular neighborhood $\Omega_{a,k}$ as in 30, and we define

$$\Omega_f := \bigcup_{k=1}^{n_f} \Omega_{a,k}.$$

We define the following sparse matrices:

$$\begin{aligned}
A: V_h &\rightarrow V'_h & A_{ij} &:= (\mathbb{C}_\Omega \nabla v_i, \nabla v_j)_\Omega, \\
K: W_h &\rightarrow W'_h & K_{ab} &:= c_\Gamma (\delta \mathbb{C}_f \nabla w_a, \nabla w_b)_\Gamma, \\
B: V_h &\rightarrow Q'_h & B_{ia} &:= (v_i|_\Gamma, w_a)_\Gamma = (v_i \circ X, w_a)_\Gamma, \\
M: W_h &\rightarrow Q'_h & M_{ab} &:= (w_a, w_b)_\Gamma.
\end{aligned} \tag{41}$$

Here B is the coupling matrix from V_h to W_h , M the mass-matrix of W_h .

After defining the vector $g_i := (b, v_i)_\Omega$, Problem 6 can be expressed in matrix form as: find $(u, w, \lambda_h) \in V_h \times W_h \times Q_h$ such that

$$\begin{pmatrix} A & 0 & B^T \\ 0 & K & -M^T \\ B & -M & 0 \end{pmatrix} \begin{pmatrix} u \\ w \\ \lambda \end{pmatrix} = \begin{pmatrix} g \\ 0 \\ 0 \end{pmatrix}. \tag{42}$$

This system has size NM^2 : computationally it is convenient to reduce its size. From the second line of the Block Matrix 42:

$$Kw = M^T \lambda = M \lambda \Rightarrow \lambda = M^{-1} Kw.$$

Then System 42 becomes:

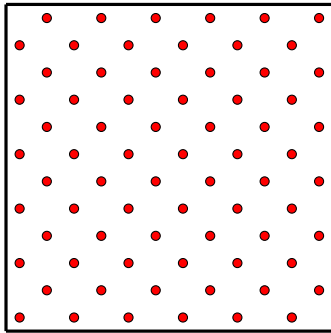
$$\begin{pmatrix} A & B^T M^{-1} K \\ B & -M \end{pmatrix} \begin{pmatrix} u \\ w \end{pmatrix} = \begin{pmatrix} g \\ 0 \end{pmatrix}. \tag{43}$$

We remove w using the equation $Bu = Mw \Rightarrow w = M^{-1}Bu$ and obtaining:

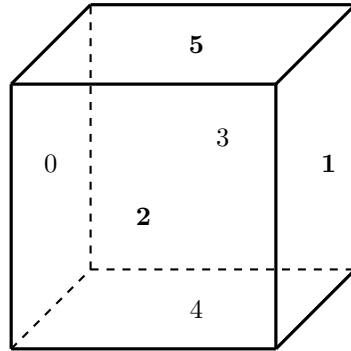
$$(A + B^T M^{-1} K M^{-1} B)u = (A + P_\Gamma^T K P_\Gamma)u = g, \tag{44}$$

where $P_\Gamma := M^{-1}B$. Boundary conditions are imposed weakly, using Nitsche method (as in [46]).

4.1. Model description



(a) Section with homogeneous fibers.



(b) Ω 's faces numbering

The elastic matrix we consider in our tests is the unitary cube $\Omega := [0, 1]^3$. All considered meshes are only uniformly refined hexaedral meshes, and we use only linear finite elements.

The elastic tensors used are described in Equations 22 – 24; for the model description we use the following parameters:

- r_Ω : global refinements of the Ω mesh.
- r_Γ : global refinements of the Γ mesh.
- $\lambda_\Omega, \mu_\Omega$: Lamé parameters for the elastic matrix.
- λ_f, μ_f : Lamé parameters for the fibers.
- β : fiber volume ratio or representative volume element (RVE), i.e., $\beta = |\Omega_f|/|\Omega|$.
- a : the radius of the fibers.

For the boundary conditions we refer to Figure 3b.

4.2. Homogeneous fibers

In our first test we consider a unidirectional composite, where fibers are uniform in properties and diameter, continuous, and parallel throughout the composite Ω (see Figure 3a).

We compare the results obtained with our model with the ones obtained using the Rule of Mixtures [18, 2], which agrees with experimental tests especially for tensile loads, and when the fiber ratio β is small.

The composite stress-strain equation, under the condition $u|_{\Omega_f} = w$, is:

$$S[u, w] = \frac{1}{2}(\mathbb{C}_\Omega Eu, Eu)_\Omega + \frac{1}{2}(\delta \mathbb{C}_f Ew, Ew)_{\Omega_f}.$$

Using the Rule of Mixtures we can approximate the integral over Ω_a with one over Ω :

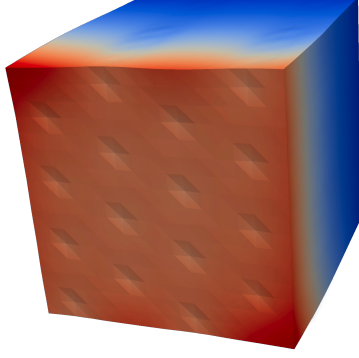
$$(\delta \mathbb{C}_f Ew, Ew)_{\Omega_f} \approx \beta(\delta \mathbb{C}_f Eu, Eu)_\Omega,$$

obtaining:

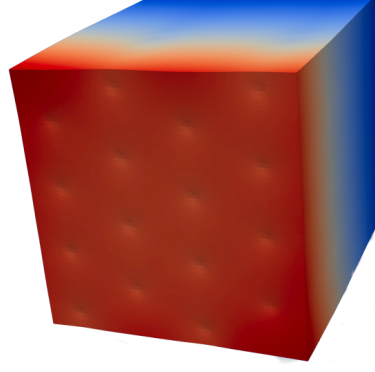
$$S[u] = \frac{1}{2}(\mathbb{C}_\Omega Eu, Eu)_\Omega + \beta \frac{1}{2}(\delta \mathbb{C}_f Eu, Eu)_\Omega. \quad (45)$$

Multiple tests were run, keeping β constant, while increasing the fiber density and reducing the fiber diameter; we expect this process to render the coupled model solution increasingly close to the homogenized one.

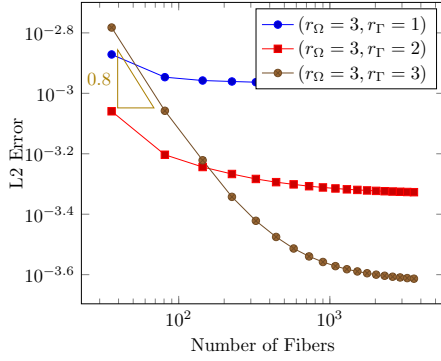
Comparing solutions. Figures 4a and 4b illustrate the influence of Ω 's refinement on the final result, when using few fibers on a pull test. Stiff fibers oppose being stretched, deforming the elastic matrix Ω through the non-slip condition: near each fiber, the deformation of Ω should be symmetrical, resembling a cone. This effect is better described in Figure 4b, where the higher value of r_Ω results in greater geometrical flexibility of the elastic matrix, allowing a better description of the effect of each fiber. Lower values of r_Ω result in a non symmetrical solution, as in Figure 4a. The lower geometrical flexibility results in an “averaged” solution which, in the case of few fibers, is closer to the homogenized model.



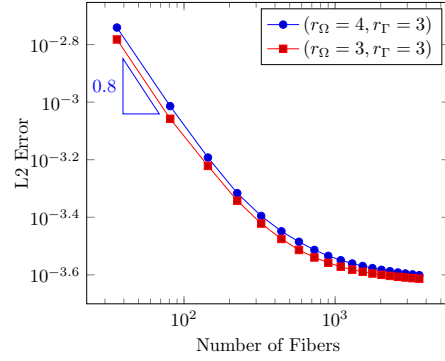
(a) Pull test example, with $r_\Omega = 4$



(b) Pull test example, with $r_\Omega = 6$



(a) Pull Test, $\lambda = \lambda_F = 0.4, \mu = 1, \mu_F = 1000, \beta = 0.1$.



(b) Pull Test, $\lambda = \lambda_F = 0.4, \mu = 1, \mu_F = 1000, r_\Omega = 3, r_\Gamma = 3$.

Figure 5: Pull tests with varying refinements.

Pull test along fibers. Dirichlet homogeneous conditions is applied to face 0, Neumann homogeneous conditions is applied to faces 2, 3, 4, 5. In the Push Test, the Neumann condition 0.05 is applied to face 1. For the Pull Test, the value -0.05 is applied to the same face. Boundary conditions are applied only to $\partial\Omega$; the fibers interact through the coupling with the elastic matrix.

We report here only data from pull tests, as push tests gave comparable results.

The use of the projection matrix $P_\Gamma: V_h \rightarrow W_h$, and the error estimate for the fully three-dimensional case (Inequality 29), both suggest that the solution quality on the elastic matrix depends on both V_h and W_h . This is apparent in Figure 5a, where for $r_\Gamma = 1$ the mesh of Γ is unable to describe the stretch of the material, resulting in the error remaining approximately constant after a certain fiber density is reached. A similar behaviour emerges in the case $r_\Gamma = 2$.

In a similar manner Figure 5b shows that refining only the elastic matrix does not

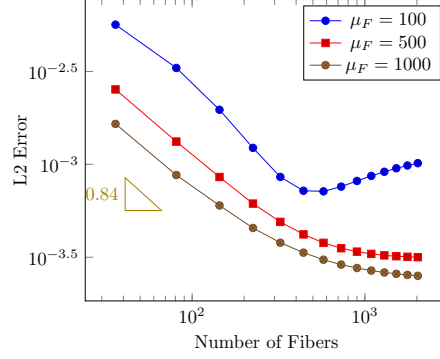


Figure 6: Pull Test with varying μ_F , $\lambda = \lambda_F = 0.4$, $\mu = 1$, $\beta = 0.1$, $r_\Omega = 3$, $r_\Gamma = 3$

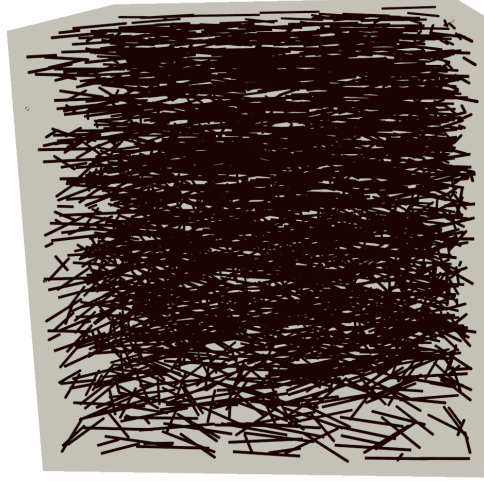


Figure 7: Random Fibers Disposition

improve the solution quality: as the number of fibers increases, the error converges to approximately the same value, which is limited by r_Γ .

Figure 6 shows an error comparison as the value of μ_F varies: as expected our model is better suited for stiff fibers.

4.3. Random fibers

Our second test is a pull test on a more complex model: a random chopped fiber reinforced composite.

We distribute small fibers at a random point of Ω , with a random direction parallel to the $\langle x, y \rangle$ plane; the fibers share the same size and properties. If a fiber surpasses the edge of Ω , it is cut.

Fiber length	0.6	0.4	0.3	0.25	0.225	0.2	0.18
Fiber radius	0.03	0.02	0.015	0.0125	0.01125	0.01	0.009
Number of Fibers	79	268	637	1100	1509	2149	2947

Table 1: Fiber Parameters

For more details on the algorithm used to distribute the fibers see the Random Sequential Adsorption algorithm [42]; our implementation generates only the plane angle, and does not implement an intersection-avoidance mechanism.

As a comparison model, we estimate the material parameters using the empirical Halpin-Tsai equations (see [17], or appendix Appendix B), and compare the results of pull-tests as done in the previous section.

Our test setting runs on the unitary cube, with a fiber ratio $\beta = 0.135$ and a fiber aspect ratio of $\frac{l}{2r} \approx 10$, where l is the fiber's length and r is the fiber's radius; the values used are described in Table 1.

We could not find an exact estimate of the error convergence, but we expect the solution to improve as the number of fibers increases because:

- the fiber radius a reduces, improving of the average non-slip condition,
- more fibers result in a more homogeneous material on the planes parallel to the $\langle x, y \rangle$ plane.

Following [42], we consider a short fiber E-glass/urethane composite: the fiber and matrix Young's modulus are, respectively, $E_f = 70GPa$ and $E_m = 3GPa$, while the Poisson ratios are $\nu_f = 0.2$ and $\nu_m = 0.38$. These values were converted to the Lamé parameters using the classic formulas for hyper elastic materials.

The predicted parameters for the composite are: $E_C = 2.20GPa$ and $\nu_C = 0.38GPa$; these are slightly different from [42] because, in the Halpin-Tsai equations, l/d was used instead of $2l/d$, see Appendix B. The boundary conditions used for the pull tests are the same of Paragraph 4.2.

We limit the global refinements of Γ , in order to obtain cells of approximately the same size on both Ω and the fibers. The results are shown in Figure 8: as the number of fiber increases the error reduces, but because the random fiber model is more complex than the homogeneous one, the final error achieved is higher than the one reached in the previous test.

5. Conclusions

Starting from a linearly elastic description of bi-phasic materials, we derive a new formulation for fiber reinforced materials where independent meshes are used to discretize the fibers and the elastic matrix, and the coping between the two phases is obtained via a distributed Lagrange multiplier.

We prove existence and uniqueness of a solution for the final saddle point problem, and we analyze a simplified model where fibers are discretised as one-dimensional.

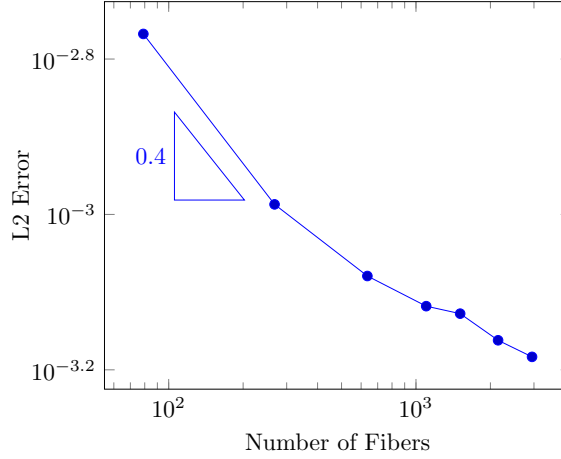


Figure 8: Random Pull Test with one dimensional approximation; global refinement of Ω : 4, global refinement of Γ : 2.

The model is validated against the Rule of Mixtures and the Hapin-Tsai equations, where we test our discretisation with uniform and random distributions of fibers. The true benefit of our model, however, lies in the possibility to tackle complex and intricate fiber structures independently from the background elastic matrix discretization, opening the way to the efficient simulation of complex multi-phase materials.

From the numerical analysis point of view, there are some issues that deserve further development, such as studying the effects of the operator B on the final error, finding better preconditioners for the final system, and exploring different coupling operators for the one dimensional coupling operator.

The formulation of our method makes it particularly suited for extensions to more complex situations, e.g., three-phasic materials, or materials where no-slip is replaced by other, more realistic conditions.

Acknowledgements

The authors would like to thank Dr. Giovanni Noselli, Dr. Davide Riccobelli, and Maicol Caponi for their priceless suggestions and insights in their fields of expertise.

Appendix A. Average non-slip condition

The following (technical) proposition shows that the element defined in Equation 34 is an element of W_Γ .

Proposition Appendix A.1. *Let $u \in \hat{V}$, then $\bar{u} \in W_\Gamma$*

Proof. Using the diffeomorphism of Ω , it is sufficient to prove that $\Phi(\bar{u})$ is $H^1(\Phi(\Omega_a))$.

Let (x, y, z) be the coordinates; $u \in V, w \in W, \phi \in C_c^\infty(\Gamma), \rho \in C_c^\infty(D_a(0))$. Since $\hat{\phi} := \phi(x)\rho(y, z) \in C_c^\infty(\Omega_a)$, using the definition of Sobolev function:

$$\int_{\Omega_a} u(x, y, z) \frac{\partial \hat{\phi}(x, y, z)}{\partial x} dx dy dz = \int_{\Omega_a} \frac{\partial u(x, y, z)}{\partial x} \hat{\phi}(x, y, z) dx dy dz$$

Then:

$$\int_{\Omega_a} \frac{\partial u(x, y, z)}{\partial x} \hat{\phi}(x, y, z) = \int_{\Gamma} \left[\int_{D_a(0)} \frac{\partial u(x, y, z)}{\partial x} \rho(y, z) dy dz \right] \phi(x) dx,$$

and:

$$\int_{\Omega_a} \frac{\partial u(x, y, z)}{\partial x} \hat{\phi}(x, y, z) dx dy dz = \int_{\Gamma} \left[\int_{D_a(0)} u(x, y, z) \rho(y, z) dy dz \right] \frac{\partial \phi(x)}{\partial x} dx.$$

Therefore $\int_{D_a(0)} u(x, y, z) \rho(y, z) dy dz \in H^1(\Gamma)$ with derivative $\int_{D_a(0)} \frac{\partial u(x, y, z)}{\partial x} \rho(y, z) dy dz$.

Consider now a sequence $\rho_n \in C_c^\infty(\Omega_a)$ of functions such that

$$0 \leq \rho_n \leq \rho_{n+1} \leq \dots \leq 1, \quad \text{and} \quad \text{supp}(\rho_n) \subset \text{supp}(\rho_{n+1}) \quad \forall n \in \mathbb{N}.$$

Repeating the same procedure, let $f_n := \int_{D_a(0)} u(x, y, z) \rho(y, z) dy dz \in H^1(\Gamma)$. Since $|\rho_n| \leq 1 \Rightarrow \|f_n\|_W \leq \|u\|_{\hat{V}}$. By compactness there exists $f \in W$ such that $f_n \xrightarrow{W_\Gamma} f$ and $f_n \xrightarrow{L^2(\Gamma)} f$.

Define $g := \int_{D_a(0)} u(x, y, z) dy dz$; by monotone convergence theorem, for a.e. $x \in \Gamma$ we have $f_n(x) \rightarrow g(x)$. The L^2 convergence of f_n implies convergence almost everywhere, therefore $g = f$ a.e., which implies $g = |D_a(0)|\bar{u} \in W$. \square

Appendix B. Halpin-Tsai equations

We report here the Halpin-Tsai equations for longitudinal moduli, as described in [2]. The fibers have length l , diameter d , the fiber and the matrix Young moduli are E_f and E_m respectively, β is the volume fraction occupied by the fibers.

We define two empirical constants:

$$\eta_L = \frac{(E_f/E_m) - 1}{(E_f/E_m) + (2l/d)}, \quad (\text{B.1})$$

$$\eta_T = \frac{(E_f/E_m) - 1}{(E_f/E_m) + 2}. \quad (\text{B.2})$$

This allows to compute the longitudinal and transverse moduli for aligned short fibers:

$$E_L = \frac{1 + (2l/d)\eta_L\beta}{1 - \eta_L\beta}, \quad (\text{B.3})$$

$$E_T = \frac{1 + 2\eta_T\beta}{1 - \eta_T\beta}. \quad (\text{B.4})$$

If fibers are randomly oriented in a plane the following equations can be used to predict the elastic modulus:

$$E_C = \frac{3}{8}E_L + \frac{5}{8}E_T, \quad (\text{B.5})$$

$$\mu_C = \frac{1}{8}E_L + \frac{1}{4}E_T. \quad (\text{B.6})$$

Since a random fiber composite is considered isotropic in its plane, the Poisson's ratio can be calculated as:

$$\nu_R = \frac{E_C}{2\mu_C} - 1. \quad (\text{B.7})$$

The properties of this composite do not depend directly on the fiber length or radius, but on the aspect ratio l/d .

Bibliography

- [1] D. F. Adams and D. R. Doner. Transverse normal loading of a unidirectional composite. *Journal of composite Materials*, 1(2):152–164, 1967.
- [2] B. D. Agarwal, L. J. Broutman, and K. Chandrashekhara. *Analysis and performance of fiber composites*. John Wiley & Sons, 2017.
- [3] G. Alzetta, D. Arndt, W. Bangerth, V. Boddu, B. Brands, D. Davydov, R. Gassmoeller, T. Heister, L. Heltai, K. Kormann, M. Kronbichler, M. Maier, J.-P. Pelteret, B. Turcksin, and D. Wells. The deal.II library, version 9.0. *Journal of Numerical Mathematics*, 26(4):173–183, 2018.
- [4] W. Bangerth, R. Hartmann, and G. Kanschat. deal.II – a general purpose object oriented finite element library. *ACM Trans. Math. Softw.*, 33(4):24/1–24/27, 2007.
- [5] R. Barrage, S. Potapenko, and M. A. Polak. Modelling transversely isotropic fiber-reinforced composites with unidirectional fibers and microstructure. *Mathematics and Mechanics of Solids*, page 1081286519838603, 2019.
- [6] T. Behzad and M. Sain. Finite element modeling of polymer curing in natural fiber reinforced composites. *Composites Science and Technology*, 67(7-8):1666–1673, 2007.
- [7] D. Boffi, F. Brezzi, M. Fortin, et al. *Mixed finite element methods and applications*, volume 44. Springer, 2013.
- [8] D. Boffi and L. Gastaldi. A finite element approach for the immersed boundary method. *Computers & structures*, 81(8-11):491–501, 2003.
- [9] D. Boffi and L. Gastaldi. A fictitious domain approach with lagrange multiplier for fluid-structure interactions. *Numerische Mathematik*, 135(3):711–732, 2017.
- [10] D. Boffi, L. Gastaldi, L. Heltai, and C. S. Peskin. On the hyper-elastic formulation of the immersed boundary method. *Computer Methods in Applied Mechanics and Engineering*, 197(25-28):2210–2231, 2008.
- [11] C. D’Angelo. Finite element approximation of elliptic problems with dirac measure terms in weighted spaces: applications to one-and three-dimensional coupled problems. *SIAM Journal on Numerical Analysis*, 50(1):194–215, 2012.
- [12] C. D’Angelo and A. Quarteroni. On the coupling of 1d and 3d diffusion-reaction equations: application to tissue perfusion problems. *Mathematical Models and Methods in Applied Sciences*, 18(08):1481–1504, 2008.
- [13] K. S. Eloh, A. Jacques, and S. Berbenni. Development of a new consistent discrete green operator for fft-based methods to solve heterogeneous problems with eigenstrains. *International Journal of Plasticity*, 116:1–23, 2019.
- [14] V. Girault and R. Glowinski. Error analysis of a fictitious domain method applied to a dirichlet problem. *Japan Journal of Industrial and Applied Mathematics*, 12(3):487, 1995.
- [15] M. E. Gurtin. *An Introduction to Continuum Mechanics*. Mathematics in Science and Engineering 158. Academic Press, 1981.
- [16] P. Hajlasz. Sobolev spaces on metric-measure spaces. *Heat kernels and analysis on manifolds, graphs, and metric spaces, (Paris, 2002)*, 2003.

- [17] J. C. Halpin and J. Kardos. The halpin-tsai equations: a review. *Polymer engineering and science*, 16(5):344–352, 1976.
- [18] Z. Hashin. On elastic behaviour of fibre reinforced materials of arbitrary transverse phase geometry. *Journal of the Mechanics and Physics of Solids*, 13(3):119–134, 1965.
- [19] Z. Hashin. *Theory of fiber reinforced materials*. NASA, Washington, United States, 1972.
- [20] Z. Hashin. Analysis of composite materials—a survey. *Journal of Applied Mechanics*, 50(3):481–505, 1983.
- [21] L. Heltai. On the stability of the finite element immersed boundary method. *Computers & Structures*, 86(7-8):598–617, 2008.
- [22] L. Heltai and A. Caiazzo. Multiscale modeling of vascularized tissues via non-matching immersed methods.
- [23] L. Heltai and F. Costanzo. Variational implementation of immersed finite element methods. *Computer Methods in Applied Mechanics and Engineering*, 229–232, 2012.
- [24] L. Heltai and N. Rotundo. Error estimates in weighted sobolev norms for finite element immersed interface methods. *Computers and Mathematics with Applications*, 2019. To appear.
- [25] G. A. Holzapfel et al. Biomechanics of soft tissue. *The handbook of materials behavior models*, 3:1049–1063, 2001.
- [26] G. A. Holzapfel and T. C. Gasser. A viscoelastic model for fiber-reinforced composites at finite strains: Continuum basis, computational aspects and applications. *Computer methods in applied mechanics and engineering*, 190(34):4379–4403, 2001.
- [27] G. A. Holzapfel, T. C. Gasser, and R. W. Ogden. A new constitutive framework for arterial wall mechanics and a comparative study of material models. *Journal of elasticity and the physical science of solids*, 61(1-3):1–48, 2000.
- [28] P. A. Huijing. Muscle as a collagen fiber reinforced composite: a review of force transmission in muscle and whole limb. *Journal of biomechanics*, 32(4):329–345, 1999.
- [29] K. Iizuka, M. Ueda, T. Takahashi, A. Yoshimura, and M. Nakayama. Development of a three-dimensional finite element model for a unidirectional carbon fiber reinforced plastic based on x-ray computed tomography images and the numerical simulation on compression. *Advanced Composite Materials*, 28(1):73–85, 2019.
- [30] T. Konopczyński, D. Rathore, J. Rathore, T. Kröger, L. Zheng, C. S. Garbe, S. Carmignato, and J. Hesser. Fully convolutional deep network architectures for automatic short glass fiber semantic segmentation from ct scans. *arXiv preprint arXiv:1901.01211*, 2019.
- [31] S. K. Kyriacou, J. D. Humphrey, and C. Schwab. Finite element analysis of nonlinear orthotropic hyperelastic membranes. *Computational Mechanics*, 18(4):269–278, Jul 1996.
- [32] G. A. L. Heltai. The deal.ii tutorial step-60: non-matching grid constraints through distributed lagrange multipliers. 2018.
- [33] Z. Lu, Z. Yuan, and Q. Liu. 3d numerical simulation for the elastic properties of random fiber composites with a wide range of fiber aspect ratios. *Computational Materials Science*, 90:123–129, 2014.
- [34] V. Lucas, J.-C. Golinval, S. Paquay, V.-D. Nguyen, L. Noels, and L. Wu. A stochastic computational multiscale approach; application to mems resonators. *Computer Methods in Applied Mechanics and Engineering*, 294:141–167, 2015.
- [35] M. Maier, M. Bardelloni, and L. Heltai. **LinearOperator** – a generic, high-level expression syntax for linear algebra. *Computers and Mathematics with Applications*, 72(1):1–24, 2016.
- [36] P. K. Mallick. *Fiber-reinforced composites: materials, manufacturing, and design*. CRC press, 2007.
- [37] J. E. Marsden and T. J. Hughes. *Mathematical foundations of elasticity*. Courier Corporation, 1994.
- [38] P. K. Mehta. *Concrete. Structure, properties and materials*. McGraw-Hill, 1986.
- [39] H. Moulinec and P. Suquet. A numerical method for computing the overall response of nonlinear composites with complex microstructure. *Computer methods in applied mechanics and engineering*, 157(1-2):69–94, 1998.
- [40] H. Moulinec and P. Suquet. Comparison of fft-based methods for computing the response of composites with highly contrasted mechanical properties. *Physica B: Condensed Matter*, 338(1-4):58–60, 2003.
- [41] T. Nakamura and S. Suresh. Effects of thermal residual stresses and fiber packing on deformation of metal-matrix composites. *Acta metallurgica et materialia*, 41(6):1665–1681, 1993.
- [42] Y. Pan, L. Iorga, and A. A. Pelegri. Analysis of 3d random chopped fiber reinforced composites using fem and random sequential adsorption. *Computational Materials Science*, 43(3):450–461,

- 2008.
- [43] C. S. Peskin. The immersed boundary method. *Acta Numerica*, 11(1):479–517, jan 2002.
 - [44] K. L. Pickering, M. A. Efendy, and T. M. Le. A review of recent developments in natural fibre composites and their mechanical performance. *Composites Part A: Applied Science and Manufacturing*, 83:98–112, 2016.
 - [45] A. C. Pipkin. Integration of an equation in membrane theory. *Zeitschrift für angewandte Mathematik und Physik ZAMP*, 19(5):818–819, Sep 1968.
 - [46] N. Rotundo, T.-Y. Kim, W. Jiang, L. Heltai, and E. Fried. Error analysis of a b-spline based finite-element method for modeling wind-driven ocean circulation. *Journal of Scientific Computing*, 69(1):430–459, 2016.
 - [47] S. Roy, L. Heltai, and F. Costanzo. Benchmarking the immersed finite element method for fluid-structure interaction problems. *Computers and Mathematics with Applications*, 69:1167–1188, 2015.
 - [48] A. Sartori, N. Giuliani, M. Bardelloni, and L. Heltai. deal2lkit: A toolkit library for high performance programming in deal.II. *SoftwareX*, 7:318–327, 2018.
 - [49] A. Zaoui. Continuum micromechanics: survey. *Journal of Engineering Mechanics*, 128(8):808–816, 2002.